ChemComm

Elastase-triggered H_2S delivery from polymer hydrogels

Journal:	*ChemComm*
Manuscript ID	CC-COM-11-2019-008752.R1
Article Type:	Communication

COMMUNICATION

Elastase-triggered H_2S delivery from polymer hydrogels

Received 00th January 20xx,
Accepted 00th January 20xx

DOI: 10.1039/x0xx00000x

Mingjun Zhou,[†a] Yun Qian,[†a] Yumeng Zhu,[a] and John Matson*[a]

We report an elastase-responsive, H_2S-releasing hydrogel prepared by covalently crosslinking a mixture of carboxymethylcellulose and poly(ethylene glycol) with an elastase-degradable peptide functionalized with an H_2S-releasing *S*-aroylthiooxime (SATO) unit. Addition of elastase triggered a gel-to-sol transition, which exposed SATOs, leading to more and longer H_2S release compared to untriggered gels.

Since the biological roles of H_2S were first discovered in 1996, its physiological functions have been investigated and explained, eventually leading to its recognition as a gasotransmitter.[1-3] Joining NO and CO in this group of endogenously produced privileged signalling molecules,[4,5] H_2S has shown potential for treating diseases due to its pro-angiogenic, antioxidant, anti-apoptotic, and anti-inflammatory properties.[6-8] Among the beneficial effects of physiological levels of H_2S, its ability to reduce inflammation is particularly intriguing given the increasing awareness of the role of inflammation in a variety of diseases, including cancer, Alzheimer's, arthritis, diabetes, stroke, and cardiovascular disease.[9] H_2S inhibits inflammation through several proposed mechanisms, including increased blood flow via vasodilation,[10] phosphodiesterase inhibition,[11] cytoprotective effects from the opening of K_{ATP} channels,[12] and as a mediator in upregulating the adherence and migration of leukocytes.[13] Due to its physiological functions, H_2S has been studied as a potential treatment for chronic diseases with recurring inflammation, such as lung disease,[14] ulcers,[15] and edemas.[16]

For many diseases, enzymes are important in their pathology, and elevated enzyme activity levels can contribute to the diagnosis of certain conditions.[17] Beyond disease detection, the ability of enzymes to selectively make and break bonds under mild conditions makes them attractive triggers in the development of responsive materials, especially for drug release.[18,19] Human neutrophil elastase (HNE) is a serine protease, secreted by neutrophils responding to inflammation.[20] Cleaving peptides/proteins selectively at the carbonyl side of Val or Ala residues, HNE has been employed as a trigger for smart materials.[21] By degrading the peptide/protein components of synthetic hydrogels, HNE can enable localized drug delivery through triggering a gel-to-sol transition.[22,23] Due to the links between inflammation, HNE, and H_2S, we became interested in developing an HNE-triggered, H_2S-releasing hydrogel, with the goal of evaluating its potential for treating chronic diseases with recurring inflammation. Such a hydrogel would ideally remain stable in the absence of inflammation, but release H_2S when HNE activity increases in response to inflammation.

We envisioned that an HNE-responsive hydrogel could be prepared by crosslinking a biocompatible polymer with HNE-degradable peptides. Peptides are convenient biodegradable building blocks for fabricating hydrogels due to their tunable chemistry and easy synthesis. Our lab has previously reported H_2S-releasing peptide hydrogels based on physical crosslinking.[24,25] However, we chose covalently crosslinked hydrogels for this project due to their stability to changes in pH and ionic strength, as well as their tunable stiffness through control of crosslinking density.[26] Only by chemically breaking the crosslinks can covalently crosslinked hydrogels be degraded. Here we describe the design and construction of peptide-crosslinked polymer hydrogels with covalently attached H_2S-donating groups. We hypothesized that degradation of the gel by HNE would initiate a gel-to-sol transition, exposing buried and unreactive H_2S-donating groups unable to react in the gel state and leading to H_2S release. Additionally, we examined the H_2S-releasing profiles of hydrogels with varying stiffnesses. Finally, we assessed their ability to protect cardiomyocytes from the harmful effects of doxorubicin (Dox).

Our synthetic route to an HNE-responsive, H_2S-releasing hydrogel is shown in Scheme 1. We started by crosslinking a 2 wt% solution of carboxymethyl cellulose (CMC) with the peptide-aldehyde **FBA-VKVKVK** (FBA = 4-formylbenzamide) using EDC/NHS coupling chemistry. However, the resulting hydrogel was quite stiff and did not undergo a gel-sol transition after exposure to HNE. To increase compliance, we lowered the amount of CMC by replacing a portion of it with poly(ethylene glycol) with carboxylic acids at each end (HOOC-PEG-COOH). We found the lowest amount of CMC required to form a robust, self-supporting gel was 35 mol% (carboxylate count, abbreviated as 35% CMC). After gelation and swelling several times to remove reaction byproducts, we analysed

[a] *Department of Chemistry and Macromolecules Innovation Institute, Virginia Tech, Blacksburg, Virginia 24061, United States. Email: jbmatson@vt.edu.*
† These two authors contributed equally.
Electronic Supplementary Information (ESI) available: [details of any supplementary information available should be included here]. See DOI: 10.1039/x0xx00000x

the rheology of this peptide-crosslinked CMC-PEG hydrogel (Fig. S2), which showed a stable storage modulus (G') of 1600 Pa at low frequencies (<5 Hz; 1% strain) with G' > G'' (G'' = loss modulus). Following lyophilization, dry hydrogel powder was reacted with *S*-benzoylthiohydroxylamine (SBTHA) to convert aldehyde groups into *S*-aroylthiooximes (SATOs), which release H_2S upon reaction with thiols such as Cys.[27] Elemental analysis of the dry SATO-hydrogel showed a sulfur loading of 1.7 wt%, corresponding to a SATO loading of 0.53 mmol/g and a near-quantitative SBTHA coupling conversion. Scanning electron microscopy (SEM) images showed no significant morphology changes between lyophilized hydrogels before and after the SBTHA coupling (Figure S6).

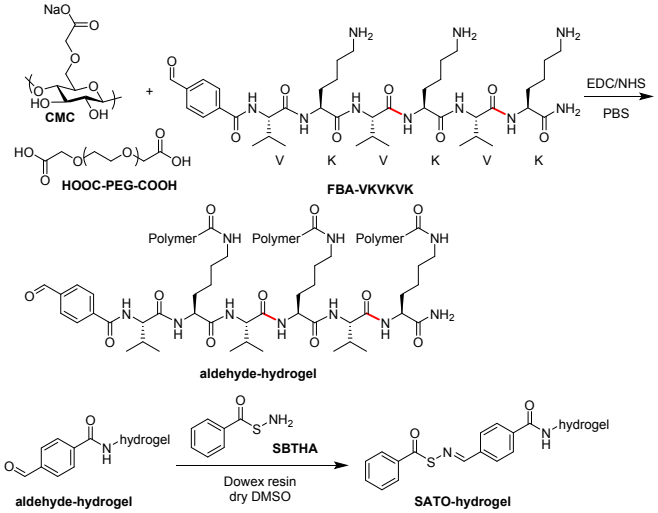

Scheme 1 Synthetic route to H_2S-releasing polymer gels. Red bonds indicate HNE cleavage sites.

We first used matrix-assisted laser desorption ionization–tandem time of flight mass spectrometer (MALDI-TOF) to investigate the degradation of the peptide-aldehyde **FBA-VKVKVK** in solution with HNE. We observed the onset of degradation within 30 min, and it continued over 24 h. As expected based on elastase specificity for Val residues, cleavage of the amide bonds on the C-terminal sides of the Val residues (red bonds in Scheme 1) occurred preferentially, although the Val amide bond closest to the N-terminus remained intact, likely due to the presence of FBA (Fig. S3).

Next, we investigated H_2S release from the SATO-hydrogel (35% CMC) with different concentrations of HNE. We used a specially designed vial with an inner well sealed with a polymer membrane, reported previously, that prevented Cys, which is added as a trigger, from interfering with the analysis of H_2S release.[28] In this type of open-air experiment using an H_2S sensitive electrode probe, the H_2S release profile reaches a maximum peaking time and peaking concentration, after which the H_2S concentration falls over time as the rate of H_2S volatilization and oxidation exceeds the rate of H_2S generation. We hypothesized that with a higher HNE concentration, the cleavage of the peptide crosslinker would accelerate, degrading the hydrogel and leading to a faster release of H_2S due to exposure of the buried SATO groups.

The release profiles and their corresponding peaking times and peaking concentrations for the 35% CMC hydrogel are shown in Fig. 1A and Table S1. Without HNE, H_2S reached a peaking concentration of 0.6±0.2 μM and a peaking time of 240±20 min. Because there is no degradation and no gel-sol transition under these conditions (Fig. S4), release in this experiment is likely from SATO groups near the hydrogel surface. With 23 μg/mL HNE (defined here as 1 unit or 1 HNE), the peaking H_2S concentration increased to 0.8±0.1 μM, with an increased peaking time of 354±4 min. The same trend applied when 2 units of HNE were added, with further increases in both of peaking concentration (1.4±0.3 μM) and peaking time (580±50 min).

We expected that more HNE would lead to faster H_2S release, indicated by a shorter peaking time, but the opposite effect was observed—more HNE led to prolonged H_2S release and in larger amounts. These results indicate that there are two types of SATO groups in the hydrogels: 1) surface SATO groups, which can be easily accessed by Cys and release H_2S; and 2) interior SATO groups, which are initially encapsulated inside the hydrogel matrix. Only by cleaving the peptide crosslinker and degrading the hydrogel are the buried SATO groups exposed to Cys. Considering the HNE degradation of the peptide crosslinker is slow based on the MALDI-TOF results (Figure S3), and the peaking time of small molecule SATOs is rather short (generally 10-80 min),[27] HNE degradation is likely the rate-determining step in H_2S release, rather than the Cys attack. Therefore, in the initial stage, the H_2S release was mostly from the surface SATO groups, which is why there was no significant difference among the three curves. However, with more HNE, a greater extent of hydrogel degradation leads to more total H_2S release. This conclusion was confirmed by visual observations, where 24 h after Cys addition, the hydrogel treated with 2 HNE was fully degraded, while the hydrogel treated with only Cys (no HNE) remained intact, and the hydrogel treated with 1 HNE was partially degraded.

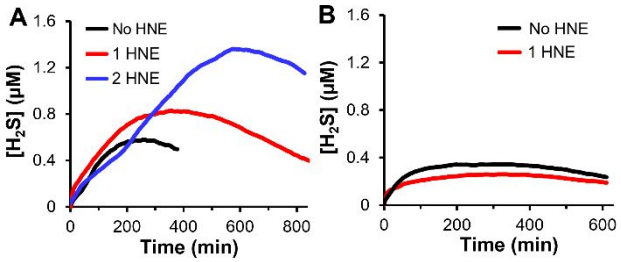

Fig. 1 H_2S-release profiles of hydrogels crosslinked with (A) HNE-degradable peptide **FBA-VKVKVK** and (B) non HNE-degradable peptide **FBA-GKGKGK**. SBTHA was added to both hydrogels to install SATO units. H_2S release experiments were performed by adding Cys (18 mM), HNE (1 HNE and 2 HNE correspond to 23 μg/mL and 46 μg/mL HNE, respectively) and PBS buffer to the gel and monitoring H_2S concentration over time.

To further confirm that the difference in the curves in Fig. 1A originated from HNE degradation, we synthesized a control hydrogel crosslinked by a non-HNE degradable peptide, **FBA-GKGKGK**, with the rest of the synthetic route unchanged. As shown in Fig. 1B, with HNE (1 unit) the release profile was even slightly lower than the one without HNE, with similar peaking times. The difference in peaking concentration is due to variability in the probe and experimental conditions. This result supports the proposed HNE degradation effect.

Based on our conclusion that there exist both surface SATO groups, which are accessible to Cys without HNE, and interior SATO groups, which only release H_2S after HNE-triggered degradation of the gel, we were interested in the H_2S-releasing behavior of these hydrogels after consuming the surface SATO groups. Thus, we designed a release experiment in which we treated a hydrogel sample only with Cys for 24 h, allowing the surface SATO groups to react completely. We then added either Cys alone or HNE and Cys. We envisioned that adding only Cys after 24 h would show no increase in H_2S concentration because all surface SATO groups would have been consumed. In contrast, we expected that adding Cys and HNE would generate more H_2S because interior SATO groups would be available to react with Cys to release H_2S after hydrogel degradation.

The results from this experiment are shown in Fig. 2A. The black curve shows the first 24 h of the experiment, when the gel was treated only with Cys. It showed a similar peaking time and concentration to the black curve shown in Fig. 1A. After 24 h, the H_2S concentration nearly reached a plateau, indicating most of the surface SATO groups were consumed. Baseline fluctuations in the instrument over several hours prevent a complete return to baseline, so H_2S release is considered complete when a plateau is reached. After 24 h, HNE (2 units) was added to the reaction mixture to trigger the gel-sol transition and expose the interior SATO groups to Cys. As shown in the blue curve, H_2S release resumed with a peaking time and concentration similar to the blue curve Fig. 1A. The pink curve, where additional Cys but no HNE was added, confirmed that the change in H_2S release was not from the addition of Cys.

Besides confirming the existence of surface and interior SATO groups, this experiment was also designed to mimic the process to treat chronic diseases with recurring inflammation. The black and pink curves mimic the process if the hydrogel was implanted into the human body at a site with no inflammation and thus low HNE activity. Even after the surface SATO groups are consumed, the hydrogel still maintained the capability to release H_2S when triggered. Upon an increase in HNE levels due to inflammation, the hydrogel can resume H_2S release to treat the disease (blue curve). Thus, the responsiveness of this hydrogel highlights its potential for treating chronic diseases with recurring inflammation.

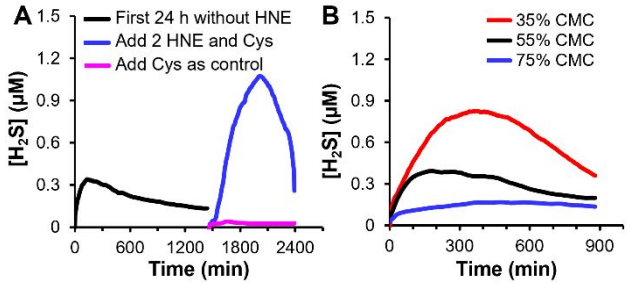

Fig. 2 H_2S-release profiles for 35% CMC hydrogel. (A) First 24 h without HNE (black curve), followed by addition of fresh Cys and 2 HNE (blue curve) and Cys (18 mM) alone as control (pink curve); (B) H_2S release profiles for hydrogels with various % of CMC treated with Cys (18 mM) and 1 HNE.

Beyond its responsiveness to HNE, we also envisioned that the hydrogel modulus could be tuned by changing the ratio of PEG to CMC. We hypothesized that more CMC in the CMC/PEG mixture would increase the hydrogel crosslinking density because of the higher number of reactive carboxylic acid groups on CMC relative to PEG. We expected that higher crosslinking densities and increased stiffness would lead to a slower response to HNE, as well as different H_2S-release profiles.

To test this hypothesis, we prepared two more hydrogels with 55 and 75 mol% CMC (carboxylate count). Rheology frequency sweep experiments showed a trend that higher % CMC in the CMC/PEG mixture led to higher G' (at low frequency, G' values of hydrogels with 55 and 75 % CMC were 1900 and 3400 Pa, respectively), indicating a higher crosslinking density with more CMC (Fig. S2).[29] After reaction with SBTHA to install SATOs, elemental analysis showed sulfur wt% values of 1.70, 1.35 and 0.44% for hydrogels with 35, 55 and 75% CMC, respectively. Therefore, gel stiffness affected conversion in the SATO formation reaction, resulting in lower SATO loadings for stiffer gels.

Increasing the CMC composition from 35 % to 55 and 75 % also affected the H_2S release peaking concentration and time (Fig. 2B) in experiments with Cys and HNE. Consistent with lower SATO loadings for stiffer gels, peaking concentrations decreased from 0.8±0.2 μM, to 0.4±0.1, and 0.24±0.04 μM, respectively. The peaking time also decreased, from 354±4 min (35% CMC) to 187±7 min (55% CMC), while the peaking time of hydrogel with 75% CMC was difficult to determine because the trace reached a plateau near 0.24 μM soon after the test began.

Finally, we evaluated the 35% CMC hydrogel in a biological assay. Our group has demonstrated the protective effects of H_2S against Dox toxicity and oxidative stress.[28,30,31] Dox, a widely used chemotherapeutic, can cause serious inflammation by damaging intestinal and mucosal barriers, inducing systemic inflammation in cancer patients treated with the drug.[32] Dox also upregulates cytokines under diabetic conditions, increasing the proinflammatory microenvironment in skeletal muscles.[33] These Dox-induced inflammatory responses also induce neutrophil production,[34,35] which increases HNE levels. Given these deleterious effects of Dox, we hypothesized that our HNE-responsive, H_2S-releasing hydrogel could show protective effects under conditions mimicking Dox-induced inflammation.

To test this hypothesis, H9C2 rat embryonic cardiomyocytes were pretreated for 1 h with 35% CMC H_2S-releasing hydrogel or controls, then Dox was added to each treatment group without removing the hydrogel or other additives. The cells

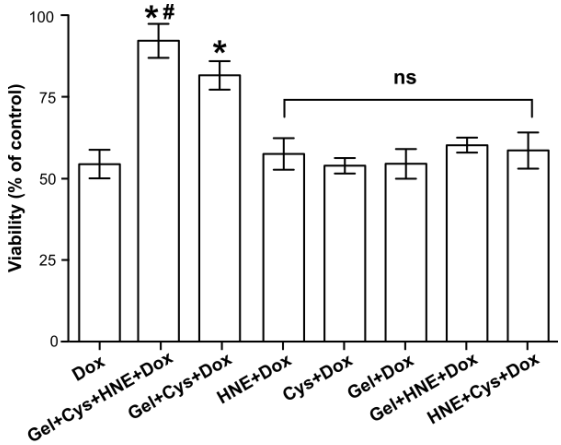

Fig. 3 Cell viability of H9C2 cardiomyocytes with different pretreatments (1 h) followed by exposure to Dox (5 μM) for 24 h. Pretreatment conditions: **Dox**; No pretreatment; **Gel+Cys+HNE+Dox**: gel (166 μM SATO groups), Cys (640 μM), HNE (8 μg/mL); **Gel+Cys+Dox**: gel (166 μM SATO groups), Cys (640 μM); **HNE+Dox**: HNE (8 μg/mL); **Cys+Dox**: Cys (640 μM); **Gel+Dox**: gel (166 μM SATO groups); **Gel+HNE+Dox**: gel (166 μM SATO groups), HNE (8 μg/mL); **Cys+HNE+Dox**: Cys (640 μM), HNE (8 μg/mL). Cell viability was measured by CCK-8. Error bars indicate standard deviations, and group comparisons were determined by a one-way analysis of variance (ANOVA) and Tukey-Kramer HSD tests (n=5, ns = not significant vs Dox; *= $p < 0.01$ vs Dox; # = $p < 0.01$ vs Gel+Cys+Dox)).

were incubated for another 24 h before analysing viability. As shown in Fig. 3, 5 μM Dox was toxic, reducing the H9C2 viability to less than 60% compared with an untreated control group. Excitingly, H_2S-releasing pretreatment groups (Gel+Cys+HNE and Gel+Cys) displayed cell viabilities of 91% and 81%, respectively. These results indicated that the H_2S-releasing hydrogel rescued H9C2 cells from Dox toxicity with or without HNE, but the effect was statistically greater with added HNE. To ensure that the protective effects were from the H_2S release, several control pretreatments were tested (HNE, Cys, Gel, Gel+HNE, and Cys+HNE), none of which released substantial amounts of H_2S. All non H_2S-releasing control groups showed low cell viabilities similar to that of the Dox only group.

In summary, in this addition to the field of H_2S-releasing materials,[36,37] we have designed and synthesized an HNE-responsive H_2S-releasing hydrogel. With more enzyme, the hydrogel released more H_2S (higher peaking concentration) over longer times (greater peaking time). The results suggest that two types of SATO groups are present in the hydrogel: SATO groups on the surface of the hydrogel that can easily react with Cys, and SATO groups buried inside the hydrogel, which are only exposed to Cys and release H_2S when the enzyme degrades the crosslinks. Based on the observed cytoprotective effect against Dox from the HNE-responsive hydrogel, we envision the potential to use HNE-responsive, H_2S-releasing hydrogels to treat chronic inflammation, where responsive materials capable of long-term H_2S delivery at the inflammatory site may reduce inflammation and related symptoms.

This work was supported by the National Institutes of Health (R01GM123508), and the National Science Foundation (DMR-1454754). We thank Ryan Carrazzone and Prof Ronit Bitton for critically reading the manuscript and Dr Keith Ray for assistance with MALDI-TOF. Mass spectrometry resources are maintained by the Virginia Tech Mass Spectrometry Incubator, operated in part by the Virginia Tech Fralin Life Science Institute.

Notes and references

1. K. Abe and H. Kimura, *J. Neurosci.*, 1996, **16**, 1066-1071.
2. R. WANG, *FASEB J.*, 2002, **16**, 1792-1798.
3. D. J. Lefer, *Proc.Natl.Acad.Sci USA*, 2007, **104**, 17907-8.
4. C. Szabó, *Nat. Rev. Drug Discovery*, 2007, **6**, 917-935.
5. C. Szabó and A. Papapetropoulos, *Br J Pharmacol*, 2011, **164**, 853-865.
6. R. C. O. Zanardo, V. Brancaleone, E. Distrutti, S. Fiorucci, G. Cirino and J. L. Wallace, *FASEB J.*, 2006, **20**, 2118-2120.
7. Y. Shen, Z. Shen, S. Luo, W. Guo and Y. Z. Zhu, *Oxid Med Cell Longev*, 2015, **2015**, 925167.
8. A. Katsouda, S.-I. Bibli, A. Pyriochou, C. Szabo and A. Papapetropoulos, *Pharmacol. Res.*, 2016, **113**, 175-185.
9. D. Wu, N. Luo, L. Wang, Z. Zhao, H. Bu, G. Xu, Y. Yan, X. Che, Z. Jiao, T. Zhao, J. Chen, A. Ji, Y. Li and G. D. Lee, *Sci. Rep.*, 2017, **7**, 455.
10. E. D. Casalini, A. G. Goodwill, M. K. Owen, S. P. Moberly, Z. C. Berwick and J. D. Tune, *Microcirculation*, 2014, **21**, 104-111.
11. M. Bucci, A. Papapetropoulos, V. Vellecco, Z. Zhou, A. Pyriochou, C. Roussos, F. Roviezzo, V. Brancaleone and G. Cirino, *Arter. Thromb. Vasc. Biol.*, 2010, **30**, 1998-2004.
12. W. Zhao, J. Zhang, Y. Lu and R. Wang, *EMBO J.*, 2001, **20**, 6008-6016.
13. M. Bhatia, *Scientifica*, **2012**, Article ID 159680.
14. Z. Wang, X. Yin, L. Gao, S. Feng, K. Song, L. Li, Y. Lu and H. Shen, *SpringerPlus*, 2016, **5**, 1084.
15. J. L. Wallace, G. Caliendo, V. Santagada, G. Cirino and S. Fiorucci, *Gastroenterology*, 2007, **132**, 261-271.
16. H. X. Zhang, S. J. Liu, X. L. Tang, G. L. Duan, X. Ni, X. Y. Zhu, Y. J. Liu and C. N. Wang, *Cell. Physiol. Biochem.*, 2016, **40**, 1603-1612.
17. Q. Hu, P. S. Katti and Z. Gu, *Nanoscale*, 2014, **6**, 12273-12286.
18. M. Zelzer, S. J. Todd, A. R. Hirst, T. O. McDonald and R. V. Ulijn, *Biomater. Sci.*, 2013, **1**, 11-39.
19. R. V. Ulijn, *J. Mater. Chem.*, 2006, **16**, 2217-2225.
20. E. K. Allan, T. L. Holyoake and H. G. Jørgensen, *Leukemia*, 2006, **20**, 2054-2055.
21. H. Ohbayashi, *Expert. Opin. Inv. Drug.*, 2002, **11**, 965-980.
22. A. A. Aimetti, M. W. Tibbitt and K. S. Anseth, *Biomacromolecules*, 2009, **10**, 1484-1489.
23. D. Kamarun, X. Zheng, L. Milanesi, C. A. Hunter and S. Krause, *Electrochim. Acta*, 2009, **54**, 4985-4990.
24. J. M. Carter, Y. Qian, J. C. Foster and J. B. Matson, *Chem. Comm.*, 2015, **51**, 13131-13134.
25. Y. Qian, K. Kaur, J. C. Foster and J. B. Matson, *Biomacromolecules*, 2019, **20**, 1077-1086.
26. K. Varaprasad, G. M. Raghavendra, T. Jayaramudu, M. M. Yallapu and R. Sadiku, *Mater.Sci Eng.C*, 2017, **79**, 958-971.
27. J. C. Foster, C. R. Powell, S. C. Radzinski and J. B. Matson, *Org. Lett.*, 2014, **16**, 1558-1561.
28. Y. Wang, K. Kaur, S. J. Scannelli, R. Bitton and J. B. Matson, *J. Am. Chem. Soc.*, 2018, **140**, 14945-14951.
29. Y. Shmidov, M. Zhou, G. Yosefi, R. Bitton and J. B. Matson, *Soft Matter*, 2019, **15**, 917-925.
30. C. R. Powell, K. M. Dillon, Y. Wang, R. J. Carrazzone and J. B. Matson, *Angew. Chem. Int. Ed.*, 2018, **57**, 6324-6328.
31. Y. Wang and J. B. Matson, *ACS Appl. Bio Mater.*, 2019, DOI: 10.1021/acsabm.9b00768.
32. L. Wang, Q. Chen, H. Qi, C. Wang, C. Wang, J. Zhang and L. Dong, *Cancer Res.*, 2016, **76**, 6631-6642.
33. R. Supriya, B. T. Tam, X. M. Pei, C. W. Lai, L. W. Chan, B. Y. Yung and P. M. Siu, *Front. Physiol.*, 2016, **7**, 323.
34. D. V. Krysko, A. Kaczmarek, O. Krysko, L. Heyndrickx, J. Woznicki, P. Bogaert, A. Cauwels, N. Takahashi, S. Magez, C. Bachert and P. Vandenabeele, *Cell Death Differ.*, 2011, **18**, 1316-1325.
35. A. Kaczmarek, O. Krysko, L. Heyndrickx, T. Løve Aaes, T. Delvaeye, C. Bachert, L. Leybaert, P. Vandenabeele and D. V. Krysko, *Cell Death Dis.*, 2013, **4**, e961.
36. M. C. Urquhart, F. Ercole, M. R. Whittaker, B. J. Boyd, T. P. Davis and J. F. Quinn, *Polym. Chem.*, 2018, **9**, 4431-4439.
37. K. Kaur, R. Carrazzone and J. B. Matson, *Antioxid. Redox Signal.*, DOI: 10.1089/ars.2019.7864.